Cluster-spin dynamics in a $GaMo_4S_8$-type compound: ^{27}Al nuclear magnetic resonance study of $AlMo_4S_8$

2007 J. Phys.: Condens. Matter 19 046206

(http://iopscience.iop.org/0953-8984/19/4/046206)

INSTITUTE OF PHYSICS PUBLISHING JOURNAL OF PHYSICS: CONDENSED MATTER

J. Phys.: Condens. Matter **19** (2007) 046206 (7pp) doi:10.1088/0953-8984/19/4/046206

Cluster-spin dynamics in a $GaMo_4S_8$-type compound: ^{27}Al nuclear magnetic resonance study of $AlMo_4S_8$

R Ikeno, H Nakamura and T Kohara

Graduate School of Material Science, University of Hyogo, Kamigori, Ako-gun, Hyogo 678-1297, Japan

Received 30 June 2006, in final form 11 December 2006
Published 12 January 2007
Online at stacks.iop.org/JPhysCM/19/046206

Abstract

The cluster-spin dynamics of the tetrahedral Mo_4 cluster, involved in $AlMo_4S_8$ with a cubic $GaMo_4S_8$ type structure, was investigated by NMR of the nonmagnetic ^{27}Al site located outside the cluster. The nuclear spin–lattice relaxation is described well by the conventional local moment model assuming the presence of $S = \frac{1}{2}$ at each cluster, indicating that each Mo_4 cluster behaves like a local spin with rigid magnitude. This behaviour is in contrast to the in-cluster relaxation, which reflects the spin-density fluctuations inside the cluster as a small unit of metal.

1. Introduction

A magnetic metal cluster implanted in a crystalline lattice is of interest as a subject of research which links the magnetism of insulating, metallic and molecular magnets. Here, a metal cluster means the assembly of a small number of transition-metal atoms in which in-cluster atoms share common d electrons to form a molecular-orbital-like cluster-orbital state. The magnetic cluster involves at least one unpaired spin in the cluster, implying that each cluster is expected to behave like a localized moment. AB_4X_8 compounds with a cubic $GaMo_4S_8$-type crystal structure (space group $F\bar{4}3m$) are known as a series of materials with magnetic metal clusters [1]. AB_4X_8 is recognized as an NaCl-type network of cubane-type ions $(B_4X_4)^{n+}$ and tetrahedral ions $(AX_4)^{n-}$. AB_4X_8 is also of interest as a related system to the spinel phase with a pyrochlore-type sublattice. The magnetism of AB_4X_8 lies between itinerant-electron and local-moment magnetism, or incorporates both characters.

Nuclear magnetic resonance (NMR) experiments, especially the measurement of relaxation, offer a powerful probe for directly investigating the dynamic aspect of electron spin interaction in magnetic materials. NMR measurements of metal clusters are seen in many papers [2], but few studies are found for *magnetic* metal clusters. In a previous paper [3], one of the present authors reported results of NMR experiments measured for the ^{51}V site in GaV_4S_8, namely the on-site NMR of the magnetic atom in the cluster. In particular, the relaxation typical of a metallic magnet was observed, i.e. the nuclear spin–lattice relaxation rate $1/T_1$ is in proportion to the d-spin susceptibility at high temperatures and decreases markedly below the structural transition associated with the reduction of the density of states at the Fermi level;

Table 1. Basic properties of $AlMo_4S_8$ and GaV_4S_8.

	$AlMo_4S_8$	GaV_4S_8
Magnetic cluster ion	$(Mo_4S_4)^{5+}$	$(V_4S_4)^{5+}$
Outermost d electron configuration	$(4d)^{11}$	$(3d)^7$
Expected spin per cluster	1/2	1/2
Crystal structure above T_S	Cubic $GaMo_4S_8$ type	Cubic $GaMo_4S_8$ type
Lattice constant at RT (Å)	9.7289 [9]	9.661 [4]
In-cluster atomic distance at RT (Å)	2.829 [9]	2.896 [4]
Intercluster distance at RT (Å)	4.051 [9]	3.936 [4]
Structural transition temperature T_S (K)	45[b]	44 [3]
Crystal symmetry below T_S	Rhombohedral	Rhombohedral
Rhombohedral angle α_{rh} (deg)	60.374 [9]	59.66 [4]
Magnetic ground state	Ferromagnetic[a]	Ferromagnetic[a]
Effective moment μ_{eff} above T_S	1.75 μ_B/Mo_4 [8]	1.45 μ_B/V_4 [3]
Weiss temperature θ above T_S (K)	6 [8]	−15.2 [3]
Weiss temperature θ below T_S (K)	18 [8]	12.6 [3]
Curie temperature T_C (K)	12[b]	13 [3]
Saturation magnetization	0.717 μ_B/Mo_4 [8]	0.80 μ_B/V_4 [4]

[a] Probably canted.
[b] Present work.

the transition to rhombohedral $R3m$ [4] was ascribed to the Jahn–Teller type instability due to cluster orbital degeneracies. The ^{51}V NMR experiment probed the spin dynamics at the in-cluster nuclear site, while the cluster-spin dynamics seen from outside appeared to be of interest. Hence, we tried to measure the relaxation at the nonmagnetic site. In experiments with GaV_4S_8 powder, however, ^{69}Ga and ^{71}Ga nuclear resonances are overlapped with the wide ^{51}V resonance in a certain temperature range, which makes the precise estimation for the relaxation time at the Ga sites difficult. Here, we select another material, $AlMo_4S_8$, to avoid such a problem; both the compounds involve metal-cluster ions with $S = \frac{1}{2}$. The basic magnetic and structural properties of $AlMo_4S_8$ [5–9] are summarized in table 1 together with those of GaV_4S_8 [3, 4]. Note that most of them are quite similar. In this paper, we first characterize the magnetism of $AlMo_4S_8$ and then discuss ^{27}Al NMR results to reveal the cluster-spin dynamics observed outside the cluster.

2. Experimental procedures

The powder sample of $AlMo_4S_8$ was prepared from pure elements by the solid state reaction in an evacuated quartz tube [5]. A single phase was confirmed by a conventional x-ray diffraction experiment. The susceptibility and magnetization were measured using a SQUID magnetometer (Quantum Design, MPMS-5). NMR was measured by the spin-echo method using a phase-coherent-type pulsed spectrometer. The nuclear spin–lattice relaxation time T_1 was measured by the saturation recovery method. For ^{27}Al (nuclear spin $I = \frac{5}{2}$), we used $\gamma/2\pi = 1.1094$ MHz kOe^{-1} as the gyromagnetic ratio.

3. Experimental results

3.1. Basic magnetic properties

Basic properties of $AlMo_4S_8$ have been reported by several authors [5–9]. Here we characterize our own sample and compare it with literature data.

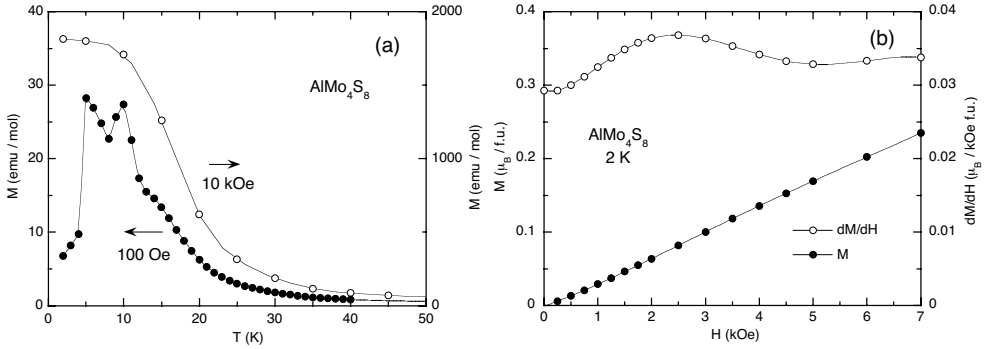

Figure 1. (a) Temperature dependences of the magnetization measured for $AlMo_4S_8$ at fields of 10 kOe and 100 Oe. (b) A low field part of the magnetization curve and its field derivative measured at 2 K.

The structural transition temperature of our sample is estimated from an anomaly in the temperature dependence of the susceptibility as $T_S \simeq 45$ K, which is comparable to those estimated by Brasen *et al* [5] (46 K) and by Rastogi [8] (50 K) but a little higher than that by Francois *et al* [9] (24 K). From the analysis of the susceptibility, we obtained values of the Weiss temperature θ and the effective paramagnetic moment $\mu_{\rm eff}$ close to those reported in the literature [8].

Figure 1(a) shows the temperature dependence of the magnetization measured at fields of 10 kOe and 100 Oe. At 10 kOe, the magnetization increases monotonically with decreasing temperature like a simple ferromagnet, while it shows a complicated temperature dependence at the low field; two peaks at 10 and 5 K and a reduction at the lower temperatures. This fact indicates that the magnetic structure in the ground state is not of the simple ferromagnet type but has antiferromagnetic components. It is highly probable for the tetrahedral cluster to have a noncollinear structure due to the anisotropy; the four atomic sites have different local symmetry axes. In $AlMo_4S_8$ it is likely that the spin direction under zero field is canted. Due to the complex behaviour at low fields, the Arrott plot did not work to determine T_C; we estimated $T_C \simeq 12$ K as the temperature where the low-field magnetization increases sharply. This transition temperature is comparable to 9.5 K reported by Brasen *et al* [5] as T_C at zero external field.

The value of saturation magnetization, estimated from the magnetization measurement up to 50 kOe at 2 K, is close to that reported by Rastogi [8]. A low-field part of the magnetization curve and its field derivative dM/dH are shown in figure 1(b). The field derivative exhibits a broad maximum at 2.5 kOe, suggesting the presence of a spin flip transition. This feature seems to be related to the complex temperature dependence of the magnetization at 100 Oe. A similar anomaly in dM/dH has been observed for powder and single-crystalline GaV_4S_8 [10].

Properties of $AlMo_4S_8$ and GaV_4S_8 are summarized in table 1. It is found that although $AlMo_4S_8$ and GaV_4S_8 have different numbers of outermost d electrons, the clusters in both the compounds have the same spin $S = \frac{1}{2}$ with nearly the same characteristic energy. (The direction of deformation at T_S is opposite, i.e. the rhombohedral angle $\alpha_{\rm rh} > 60^\circ$ for $AlMo_4S_8$ and $\alpha_{\rm rh} < 60^\circ$ for GaV_4S_8, but can be explained as being due to the difference in the number of d electrons in the clusters [4].)

3.2. Spectrum

Field-swept ^{27}Al NMR spectra were measured at the operating frequency of 65 MHz. Examples below T_S are shown in figure 2. The spectrum, centred near the zero shift position $^{27}K = 0$,

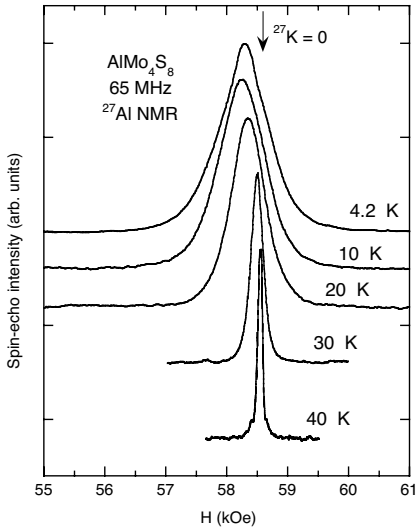

Figure 2. Examples of field-swept ^{27}Al NMR spectra of $AlMo_4S_8$ at 65 MHz and at several temperatures.

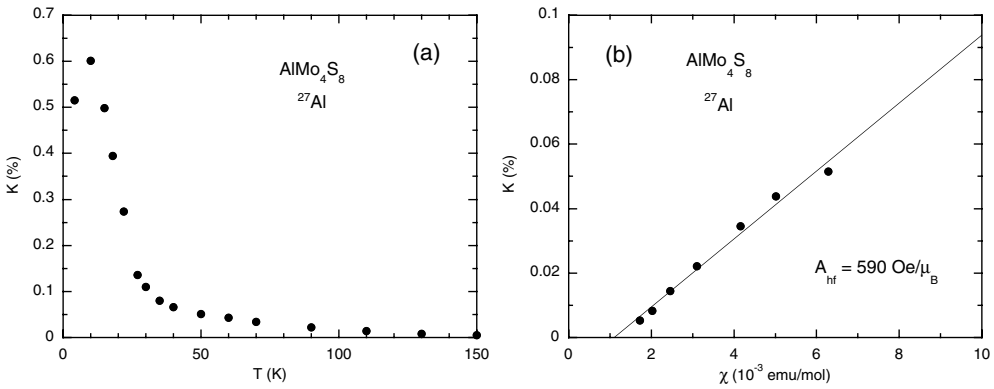

Figure 3. (a) The temperature dependence of the ^{27}Al Knight shift for $AlMo_4S_8$. (b) The $K-\chi$ plot at $T > T_S$.

is broadened gradually with decreasing temperature. Above T_S, a strong free-induction-decay signal was observed in the same experimental conditions, indicating a sharper line width, which is in accordance with the cubic local symmetry at the Al site above T_S. Although the site symmetry is lowered below T_S, the lineshape is nearly symmetric with negligible quadrupolar structure.

Figure 3(a) shows the temperature dependence of the Knight shift K, where we call all paramagnetic shifts the Knight shift regardless of their origin, estimated from the peak position of the field-swept spectra; the Al site is, in fact, not unique below T_S, hence a kind of averaged value of K is roughly estimated from the peak position due to the lack of crystallographic information and experimental resolution. The Knight shift, which is positive and small in magnitude, shows a monotonic temperature dependence above 10 K without remarkable anomaly at T_S. The Knight shift above T_S is plotted against the susceptibility

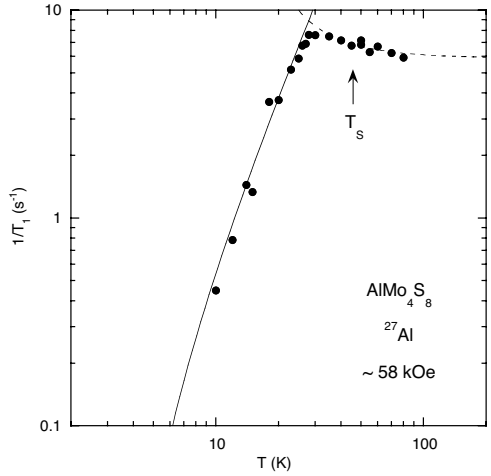

Figure 4. The temperature dependence of $1/T_1$ at the ^{27}Al site in $AlMo_4S_8$. Solid and broken curves indicates fits to the local moment model.

with the temperature as an implicit parameter in figure 3(b) (the so-called $K-\chi$ plot). The hyperfine coupling constant $A_{\rm hf}$, defined as $K = (A_{\rm hf}/N\mu_{\rm B})\chi$ with N the Avogadro number and estimated from the slope of the linear relation, is 590 Oe/$\mu_{\rm B}$. Note that, under zero field, dipolar fields coming from Mo clusters cancel out at the Al site, since Mo clusters are arranged in the cubic symmetry with respect to the Al site. The weak but finite coupling between Mo clusters and Al nuclei is probably due to the field-induced dipolar field, which is, for example, associated with the spatial asymmetry of the spin-density distribution in the Mo clusters. Although $T_{\rm C}$ cannot be defined rigorously in the external field, the ^{27}Al resonance does not shift markedly below ∼20 K where the magnetization starts to increase rapidly. The small internal field even below $T_{\rm C}$ is in accordance with the small hyperfine coupling estimated in the paramagnetic state.

3.3. Nuclear spin–lattice relaxation

The recovery curve of the ^{27}Al nuclear magnetization was reproduced by a single exponential function. Figure 4 shows the nuclear spin–lattice relaxation rate $1/T_1$ plotted against the temperature, which shows a weak dependence in the paramagnetic state and no discontinuous change at $T_{\rm S}$. This is in contrast to the case of ^{51}V-T_1 in GaV_4S_8; a discontinuous change at $T_{\rm S}$. The ^{27}Al result suggests that the magnitude of the cluster spin and the exchange interaction between clusters are not modified markedly at $T_{\rm S}$.

Since paramagnetic local moments fluctuating at random generally give the temperature-independent T_1, the behaviour of ^{27}Al-T_1 at high temperatures indicates the presence of weakly correlated paramagnetic local moments. We tentatively fit the result of $1/T_1$ in the paramagnetic region to $1/T_1 = a/(T-T_{\rm C})^{3/2} + 1/T_{1\infty}$, with a and $T_{1\infty}$ fitting parameters. The first term on the right-hand side corresponds to the critical behaviour for the ferromagnetically coupled local moments [11]. We tentatively applied this relation as one of the asymptotic forms to the critical point only to estimate $1/T_{1\infty}$; this relation is, in fact, valid only in specific conditions, i.e. under zero field and at low temperature [11], but works well qualitatively. The best fit result, shown by the broken curve in figure 4, gives $1/T_{1\infty} = 5.9$ s^{-1}. When the nuclear magnetic relaxation is dominated by fluctuations of the hyperfine field coming from

exchange-coupled local spins, by defining the hyperfine interaction as $A\vec{S}\cdot\vec{I}$, $1/T_1$ is given by

$$\frac{1}{T_1} = \frac{\sqrt{2\pi}S(S+1)A^2}{3\hbar^2\omega_{\rm ex}} \tag{1}$$

at $T \gg T_{\rm C}$, where $\omega_{\rm ex}$ is the exchange frequency given by

$$\omega_{\rm ex}^2 = \frac{2J^2}{3\hbar^2}zS(S+1), \tag{2}$$

with z the number of neighbouring spins coupled with a local spin and J the exchange integral for neighbouring spins [12]. Here we try to calculate the value assuming that the nuclear magnetization at the ^{27}Al site relaxes to thermally fluctuating Mo clusters with the rigid magnitude of spin, $S = \frac{1}{2}$. We replace $(A/\hbar)^2$ by $(2\gamma\mu_{\rm B}A_{\rm hf}/z')^2z'$ with z' the number of neighbouring Mo clusters coupled with an Al nucleus. The exchange frequency is estimated to be $\omega_{\rm ex} = 1.28$ THz from $z = 12$ and $T_{\rm C} = 12$ K by using a relation $T_{\rm C} = zJS(S+1)/3k_{\rm B}$. With $z' = 6$, $\gamma/2\pi = 1109.4$ Hz Oe^{-1} and $A_{\rm hf} = 590$ Oe/$\mu_{\rm B}$, we obtain $1/T_1 = 5.5$ s^{-1}, which is in reasonable agreement with the experimental value of $1/T_{1\infty}$.

The ferromagnetic ordering suppresses spin excitations. As an effect of the external field, $1/T_1$ starts to decrease from a temperature a little higher than $T_{\rm C}$ at zero field. Generally the nuclear magnetic relaxation in the magnetically ordered local spin system is determined more or less by spin wave excitations. When the dipolar field $H_{\rm dip}$ is induced by an external field, the relaxation rate at the nonmagnetic site is given by

$$\frac{1}{T_1} = \frac{2(\gamma H_{\rm dip})^2}{15\pi\omega_{\rm ex}}\left(\frac{k_{\rm B}T}{\hbar\omega_{\rm ex}}\right)^2 \ln\left(\frac{k_{\rm B}T}{2\mu_{\rm B}H_{\rm A}}\right), \tag{3}$$

with $H_{\rm A}$ the anisotropic field [13]. Note that this anisotropy is of the cluster spin, not within the cluster discussed in section 3.1. The fitting of the low-temperature part to this type of equation, $1/T_1 = bT^2\ln(T/c)$ with b and c the fitting parameters, is shown by the solid curve in figure 4. The best fit result gives $b = 0.0058$ s^{-1} K^{-2} and $c = 3.9$ K. By replacing $(\gamma H_{\rm dip})^2$ with $(2\gamma\mu_{\rm B}A_{\rm hf}/z')^2z'$, the value of b is tentatively calculated from experimental values of $A_{\rm hf}$ and $\omega_{\rm ex}$ to be 0.0039 s^{-1} K^{-2}, which is in reasonable agreement with the experimental value. As above, the relaxation of the nonmagnetic ^{27}Al site in $AlMo_4S_8$ is reasonably explained by the relaxation to thermally fluctuating Mo clusters with $S = \frac{1}{2}$.

4. Conclusion

We have measured the nuclear spin–lattice relaxation at the ^{27}Al site in $AlMo_4S_8$ to probe the cluster-spin dynamics of the magnetic Mo_4 cluster. The relaxation is well explained by the conventional local moment model, indicating that each Mo_4 cluster looks like a local spin with rigid magnitude when seen from the nonmagnetic site outside the cluster. This is in contrast to the NMR result obtained for ^{51}V in GaV_4S_8 [3]; the in-cluster relaxation reflects spin-density fluctuations in the cluster as a small unit of metal. In other words, we have seen two different types of relaxation, i.e. both metallic and insulating behaviours in the same kind of material.

Acknowledgments

This work was supported by Grants-in-Aid for Scientific Research from the Ministry of Education, Culture, Sports, Science and Technology, Japan.

References

[1] Johrendt D 1998 *Z. Anorg. Allg. Chem.* **624** 952 see also references cited therein
[2] For a review, see for example van der Klink J J and Brom H B 2000 *Prog. Nucl. Magn. Reson. Spectrosc.* **36** 89
[3] Nakamura H, Chudo H and Shiga M 2005 *J. Phys.: Condens. Matter* **17** 6015
[4] Pocha R, Johrendt D and Pöttgen R 2000 *Chem. Mater.* **12** 2882
[5] Brasen D, Vandenberg J M, Robbins M, Willens R H, Reed W A, Sherwood R C and Pinder X J 1975 *J. Solid State Chem.* **13** 298
[6] Vandenberg J M and Brasen D 1975 *J. Solid State Chem.* **14** 203
[7] Perrin C, Chevrel R and Sergent M 1975 *C. R. Acad. Sci. Paris* C **280** 949
[8] Rastogi A K 1987 *Current Trends in the Physics of Materials* (Singapore: World Scientific) p 316
[9] Fransois M, Alexandrif O V, Yvon K, Ben Yaich-Aerrache H, Gougeon P, Potel M and Sergent M 1992 *Z. Kristallogr.* **200** 47
[10] Nakamura H, unpublished
[11] Moriya T 1962 *Prog. Theor. Phys.* **28** 371
[12] Moriya T 1956 *Prog. Theor. Phys.* **16** 23
Moriya T 1956 *Prog. Theor. Phys.* **16** 641
[13] Turov E A and Petrov M P 1972 *Nuclear Magnetic Resonance in Ferro- and Antiferromagnets* (New York: Wiley)